JOURNAL OF CATALYSIS **180,** 123–131 (1998)
ARTICLE NO. CA982263

Effects of Copper Phase on CO Oxidation over Supported Wacker-Type Catalysts

Eun Duck Park and Jae Sung Lee[1]

Department of Chemical Engineering and School of Environmental Engineering, Pohang University of Science and Technology (POSTECH), San 31 Hyoja-Dong, Pohang 790-784, Republic of Korea

Received March 5, 1998; revised August 20, 1998; accepted August 21, 1998

Effects of copper phase on oxidation of carbon monoxide over supported Wacker-type catalysts were examined. XRD patterns and XANES spectra of the catalysts were measured to determine the bulk phase and the chemical environment of copper. The catalytic activity was affected by the composition of copper precursors, the nature of supports, the presence of HCl and SO_2 in the feed, and the reaction temperature. All these variables affecting the catalytic activity influenced the XRD intensity of $Cu_2Cl(OH)_3$ phase in the same manner, which was believed to be the active copper phase of the catalyst. Thus the XRD intensity of $Cu_2Cl(OH)_3$ of a catalyst was closely correlated with its catalytic activity and the change in the catalytic activity of CO oxidation with respect to different reaction and preparation conditions was directly related to the behavior of the active copper phase with respect to those variables.

INTRODUCTION

A main air pollutant, carbon monoxide is produced from heating apparatus, transportation vehicles, and industrial stacks. Catalytic oxidation has been proved to be an efficient and economical measure for removing carbon monoxide, and various catalyst systems have been reported. Supported noble metal catalysts often require reaction temperatures higher than 473 K (1). Metal oxide catalysts such as hopcalite (2) and SnO_2–CuO (3) require temperatures much lower than 473 K, but they are easily poisoned by water vapor contained in the feed gas stream. Recently, several new catalytic systems, such as Au/metal oxide (4) and Pt/SnO_2 (5), have been reported to be highly effective for low-temperature CO oxidation even in the presence of water.

The supported Wacker catalyst, in which an aqueous solution of $PdCl_2$–$CuCl_2$ is loaded into the pores of the high-surface-area supports, is known to accelerate the oxidation of carbon monoxide at low temperatures (6–13). The catalyst exhibits high CO conversion near room temperature and is stable even in the presence of water in the feed. The overall chemistry of CO oxidation in the catalytic system is believed to be similar to that of the well-known Wacker processes in the presence of a homogeneous $PdCl_2$–$CuCl_2$ catalyst (7).

$$CO + PdCl_2 + H_2O \rightarrow CO_2 + Pd(0) + 2HCl \quad [1]$$

$$Pd(0) + 2CuCl_2 \rightarrow PdCl_2 + 2CuCl \quad [2]$$

$$2CuCl + 2HCl + 1/2O_2 \rightarrow 2CuCl_2 + H_2O \quad [3]$$

Initially, $PdCl_2$ is reduced to Pd(0) by carbon monoxide, and then Pd(0) is reoxidized to $PdCl_2$ by $CuCl_2$. CuCl formed in reaction [2] is reoxidized to $CuCl_2$ by molecular O_2, which is also incldued in the feed gas stream. The presence of water is essential to sustain this catalytic cycle as shown above and also was found experimentally to be so for supported Wacker-type catalysts (10).

The supported Wacker-type catalyst has been reported to have an unusual temperature dependence of the catalytic activity, showing a maximum around 313 K and decreasing with increasing reaction temperatures (8–11). Therefore the operation window is very narrow near ambient temperatures considering the exothermic CO oxidation reaction. Lloyd and Rowe (7) claimed that $Cu(NO_3)_2$ serves as a promoter for this catalyst when supported on alumina and used for CO oxidation. Kim *et al.* (10) examined the effect of catalyst composition and reaction conditions.

In the supported $PdCl_2$–$CuCl_2$ catalyst system, the characteristic of the supports is also a critical parameter for catalytic performance. Choi and Vannice (9) observed higher activity over hydrophobic carbon than over hydrophilic alumina. They also discussed the water effects over these two supports. Lee *et al.* (12) reported that the catalytic activity decreased approximately in the order active carbon > (active carbon + ZSM-5) > ZSM-5 > molecular sieve-13X > molecular sieve-5A > alumina. Kim *et al.* (10) reported that the activity of alumina-supported $PdCl_2$–$CuCl_2$ showed a marked dependence on the partial pressure of water, whereas the carbon-supported catalyst showed no such dependence, although its presence was still required. Choi and

---

[1] To whom correspondence should be addressed. E-mail: jlee@postech.ac.kr.

0021-9517/98 $25.00

Vannice (9) investigated the mechanism of CO oxidation in kinetic and infrared spectroscopy studies. They suggested that the active species on the catalyst surface were PdClCO, CuClCO, and possibly the Pd–Cu complex. In an X-ray absorption fine structure (XAFS) study, Lee *et al.* (13, 14) examined the $PdCl_2$–$CuCl_2/Al_2O_3$ catalysts and found that the active phase of palladium was Pd(II) species containing Cl and carbonyl ligands. Any direct interaction of Pd–Pd or Pd–Cu was not observed. The active phase of copper was suggested to be solid $Cu_2Cl(OH)_3$ particles. However, Yamamoto *et al.* (15) characterized the $PdCl_2$–$CuCl_2$ catalysts supported on activated carbon and reported that $CuCl_2$ was partially reduced by the reduction sites on the support surface to Cu(I) species coordinated with three Cl^- anions.

Recently, we found that the supported Wacker-type catalyst was resistant to organic halogen compounds at low temperatures, unlike other CO oxidation catalysts, and showed stable catalytic activity at temperatures higher than 373 K (16). This relatively high temperature range has not been intensively studied before for these catalysts. This catalyst system can play a distinct role in oxidizing CO in vent streams containing halogen impurities. In this paper, the effects of supports, $Cu(NO_3)_2$ as a promoter, and halogen compounds on supported Wacker-type catalysts are studied. In particular, the relation between the catalytic activity and the solid phase of copper is discussed.

EXPERIMENTAL

Catalyst Preparation

The catalyst was prepared by a wet impregnation method to impregnate supports with an aqueous solution of palladium and copper. The support was dried at 383 K for 12 h in an oven before impregnation. Support materials were γ-Al_2O_3 (Alfa, BET surface area, 170 m^2/g), activated carbon (Aldrich, BET surface area, 1075 m^2/g), silica (Aldrich, BET surface area, 300 m^2/g), and H-type mordenite (HM, Si/Al = 5.29, BET surface area, 449 m^2/g). The metal precursors were $PdCl_2$ (Sigma, 99.9%), $CuCl_2 \cdot 2H_2O$ (Aldrich, 99.9%), and $Cu(NO_3)_2 \cdot 3H_2O$ (Aldrich, 99.9%). Various compositions of impregnation solution were used, but a typical value was 2 wt% Pd and 12 wt% Cu (mole ratio of $CuCl_2$ to $Cu(NO_3)_2$ was 1 : 2). To prepare 5 g of catalyst on a dehydrated basis, 0.167 g $PdCl_2$, 0.535 g $CuCl_2 \cdot 2H_2O$, and 1.592 g $Cu(NO_3)_2 \cdot 3H_2O$ were dissolved in 100 ml distilled water. Then, 3.158 g support was added to this aqueous solution and evacuated at 333 K. This catalyst was dried at ambient temperature and used for the reaction without any further pretreatment.

CO Oxidation

The catalytic oxidation of carbon monoxide was examined in a fixed-bed flow reaction system under atmospheric pressure. The reactor was a 3/8-in. Pyrex tube with a sintered glass disk to hold the catalyst in the reactor. Reaction temperature was monitored by a thermocouple inserted into the center of the catalyst bed. A premixed $CO/O_2/N_2$ stream was supplied through a mass flow controller into the reactor. The feed stream was saturated with water through a saturator enclosed in a constant temperature bath and fed to the reactor. When HCl or SO_2 was fed with reactants, these gases bypassed the water saturator and were supplied into the reactor directly to avoid their dissolution in the water. The constant reaction temperature of the reactor was achieved by controlling the temperature of an electric furnace surrounding the reactor. Reactants and products were analyzed by an on-line gas chromatography (HP5890A, molecular sieve 13X column) and CO infrared analyzer (Thermo Environmental Instrument Inc.).

Characterization of Catalysts

X-ray powder diffraction patterns were obtained at room temperature using a M18XHF (MAC Science Co.) with Ni-filtered Cu$K\alpha$ radiation (1.54056 Å). The X-ray tube was operated at 40 kV and 200 mA. Samples were finely ground and packed into a glass holder having an 18 × 18 × 2-mm opening. No adhesive or binder was necessary. The 2θ angles were scanned at a rate of 4° min^{-1}.

The XANES (X-ray absorption near edge structure) spectra were taken in a transmission mode for the K-edge of Cu at beamline 3C1 of the Pohang Accelerator Laboratory (PAL) in Pohang, Korea. They were analyzed with the UWXAFS 3.0 package licensed from University of Washington (17). The standard analysis procedure is described elsewhere in detail (18).

RESULTS

Effects of Supports

The rates of CO oxidation over $PdCl_2$–$CuCl_2$ catalysts showed different bahaviors at temperatures close to room temperature (RT) and at temperatures close to 373 K. The reaction rates are expressed in moles of CO converted per mole of Pd per second. They are true turnover rates because Pd was found to be the main active component of the catalyst and to be present as a molecular species containing a single Pd atom (10, 13, 14). In Fig. 1, the rates are compared on various supports at three typical temperatures of 318, 373, and 423 K. At 318 K, carbon was clearly superior to other supports tested both in activity and in its maintenance. The turnover rate value at 318 K is similar to that reported by Choi and Vannice (9) at RT over carbon-supported $PdCl_2$–$CuCl_2$ catalysts. The stable CO conversion was achieved over Al_2O_3 as well. However, the activity of silica- and HM-supported catalysts decreased rapidly with time on stream. At high

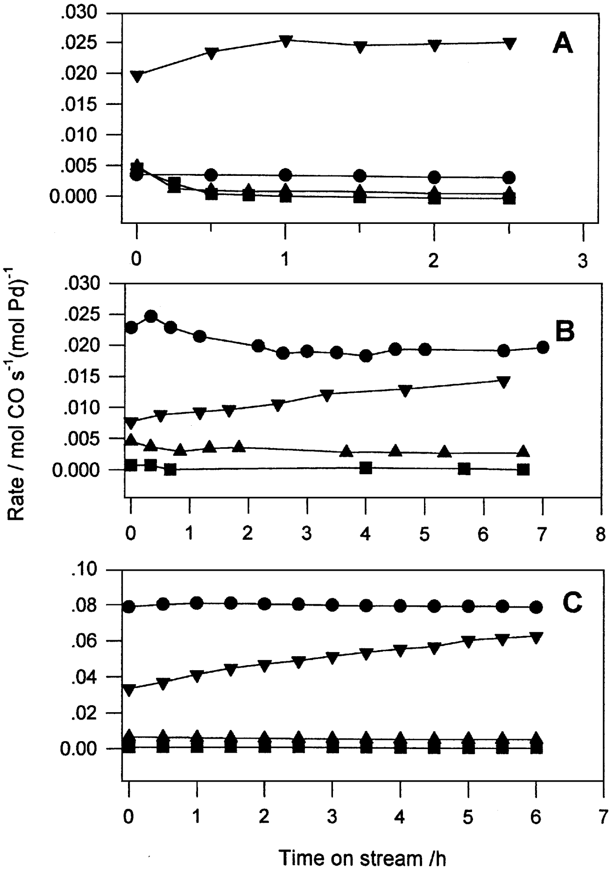

FIG. 1. The rate of CO oxidation over supported $PdCl_2$–$CuCl_2$ catalysts containing 2 wt% Pd and 12 wt% Cu at temperatures of 318 K (A), 373 K (B), and 423 K (C). The reactants, CO, O_2, and H_2O, were fed to the catalyst at concentrations of 1, 10, and 2.3 vol% each in nitrogen: ●, Al_2O_3; ■, silica; ▲, HM; and ▼, carbon.

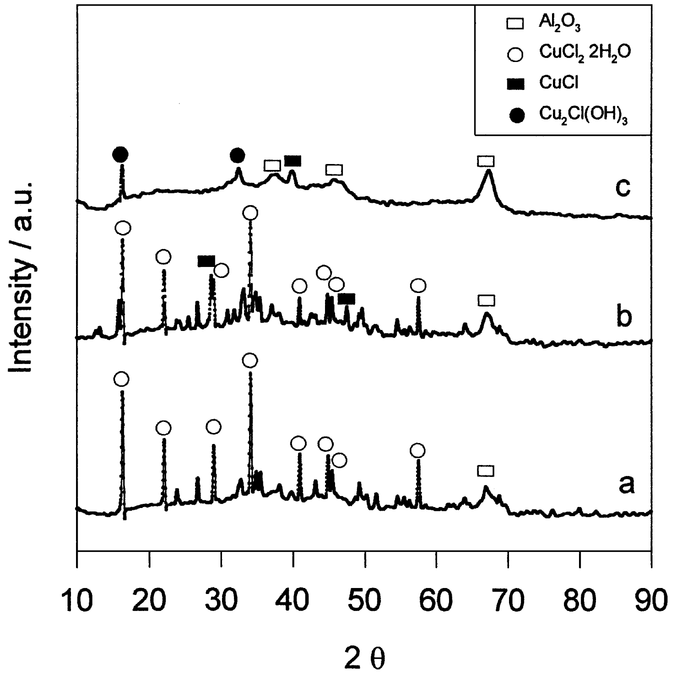

FIG. 2. X-ray diffractogram of $PdCl_2$–$CuCl_2$/Al_2O_3 catalysts before reaction (a), after reaction at 318 K (b), and after reaction at 423 K (c).

temperatures, carbon and alumina were again effective supports. However, carbon-supported catalyst started at a rate lower than that of alumina-supported catalyst, yet the rate increased steadily with reaction time. The XRD patterns of Al_2O_3-supported catalyst are shown in Fig. 2. $CuCl_2 \cdot 2H_2O$ was a dominant solid phase before reaction, and a part of it transformed into CuCl after reaction at 318 K. However, $CuCl_2 \cdot 2H_2O$ changed into $Cu_2Cl(OH)_3$ after reaction at 423 K, the temperature at which this catalyst showed the highest rate of CO oxidation among four catalysts with different supports. For silica-supported catalysts, $CuCl_2 \cdot 2H_2O$ phase transformed into the CuCl phase after reaction at all temperatures tested, as shown in Fig. 3. Carbon-supported catalysts showed $CuCl_2 \cdot 2H_2O$ and $Cu_2Cl(OH)_3$ phases before the reaction, as shown in Fig. 4. A part of $CuCl_2 \cdot 2H_2O$ transformed to $Cu_2Cl(OH)_3$ after reaction at 318 K, and the transformation was almost complete after reaction at 423 K. Hence, it is evident that different behaviors of $PdCl_2$–$CuCl_2$ catalysts supported on different materials correlate well with their solid copper phases; catalysts showing strong XRD peaks of $Cu_2Cl(OH)_3$ show high activities of CO oxidation.

Effects of $Cu(NO_3)_2$ as a Promoter

$Cu(NO_3)_2$ was added as an additional copper precursor to carbon-supported $PdCl_2$–$CuCl_2$ catalyst, and its activity of

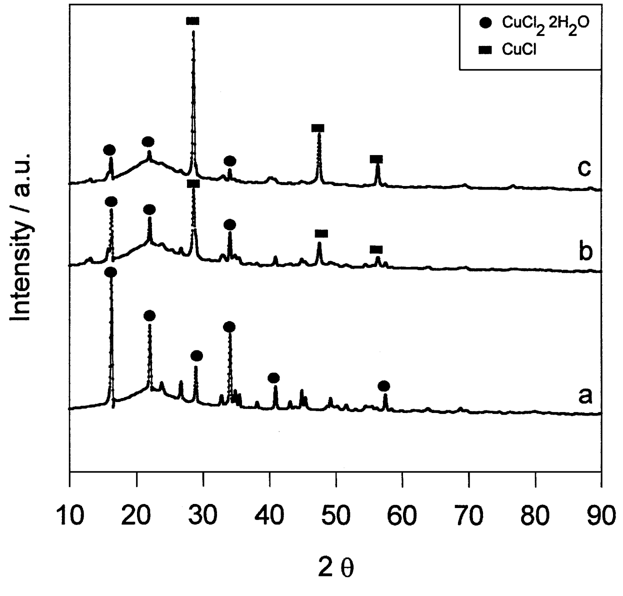

FIG. 3. X-ray diffractogram of $PdCl_2$–$CuCl_2$/silica catalysts before reaction (a), after reaction at 318 K (b), and after reaction at 423 K (c).

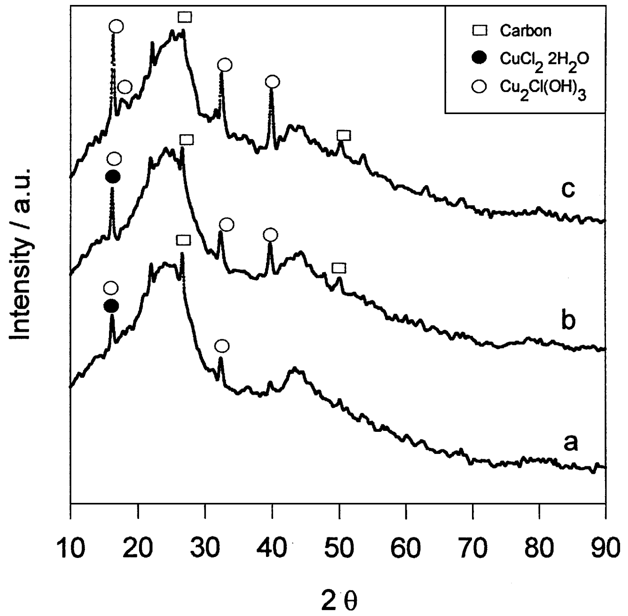

FIG. 4. X-ray diffractogram of $PdCl_2$–$CuCl_2$/carbon catalysts before reaction (a), after reaction at 318 K (b), and after reaction at 423 K (c).

CO oxidation is shown in Fig. 5. At 303 and 318 K, there was an induction period for the $PdCl_2$–$CuCl_2$–$Cu(NO_3)_2$ catalyst to reach a steady state, and the CO conversion over this catalyst at steady state was ca. 50% higher than that over the $PdCl_2$–$CuCl_2$ catalyst. At temperatures of 373 and 423 K, the induction period disappeared and its activity decreased slightly before reaching a steady-state value. XRD patterns of this catalyst system are shown in Fig. 6. This catalyst had the $Cu_2Cl(OH)_3$ phase before reaction (Fig. 6a) and its peak intensity increased with reaction time at 303 K (Fig. 6c), in line with the increase in activity of CO oxidiation. The initial decrease in catalytic activity at the high temperature can also be explained by the decreased peak intensity of the $Cu_2Cl(OH)_3$ phase after reaction at 373 K, as shown in Fig. 6b.

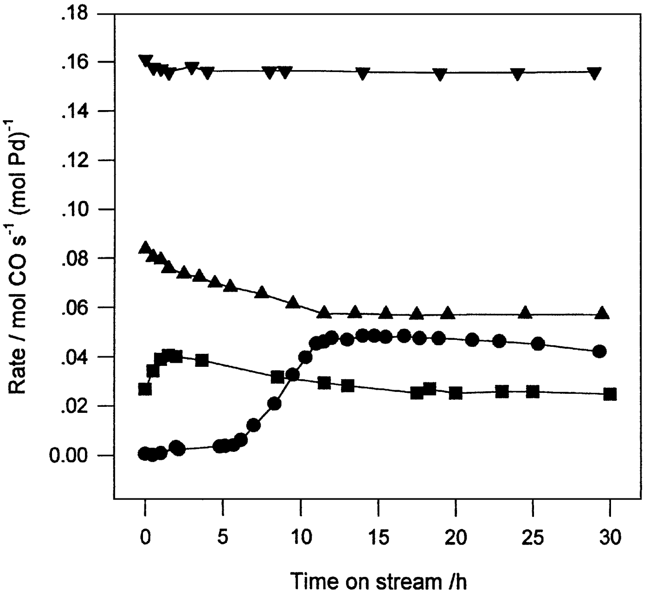

FIG. 5. The rate of CO oxidation over $PdCl_2$–$CuCl_2$–$Cu(NO_3)_2$/carbon catalyst containing 2 wt% Pd and 12 wt% Cu($[CuCl_2]:[Cu(NO_3)_2] = 1:2$) at temperatures of 303 K (●), 318 K (■), 373 K (▲), and 423 K (▼). The reactants, CO, O_2, and H_2O, were fed to the catalyst at a concentration of 1, 10, and 2.3 vol% each in nitrogen.

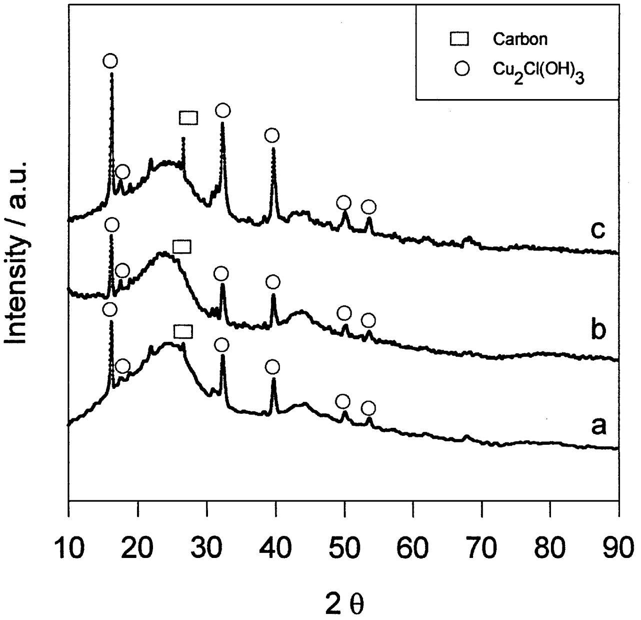

FIG. 6. X-ray diffractogram of $PdCl_2$–$CuCl_2$–$Cu(NO_3)_2$/carbon catalysts before reaction (a), after reaction at 373 K (b), and after reaction at 303 K (c).

For the Al_2O_3-supported $PdCl_2$–$CuCl_2$–$Cu(NO_3)_2$ catalyst, the reaction pattern observed differed from that of the carbon-supported catalyst, as shown in Fig. 7. The catalytic activity decreased with time at 318 K and increased at 373 K. XRD patterns of this catalyst shown in Fig. 8 indicate that $Cu_2Cl(OH)_3$, which was the dominant phase before reaction (Fig. 8a), transformed into CuCl at 318 K (Fig. 8c), whereas this CuCl phase was not formed after reaction at high temperature (Fig 8b).

The rates of CO oxidation and XRD patterns of a carbon-supported $PdCl_2$–$Cu(NO_3)_2$ catalyst without $CuCl_2$ are shown in Figs. 9 and 10. This catalyst showed activities substantially lower than those of the $PdCl_2$–$CuCl_2$–$Cu(NO_3)_2$/carbon catalysts. At 303 K, the catalytic activity increased at first and reached a steady-state value. This activity pattern was related to the increased peak intensity of $Cu_2Cl(OH)_3$, as shown in Fig. 10b. At 423 K, $Cu(NO_3)_2$ decomposed into CuO and the catalytic activity decreased (Fig. 10c). Again, the promotional effect of $Cu(NO_3)_2$ addition and the induction period observed for this catalyst at low temperatures are nicely accounted for by the formation of the well-defined $Cu_2Cl(OH)_3$ phase.

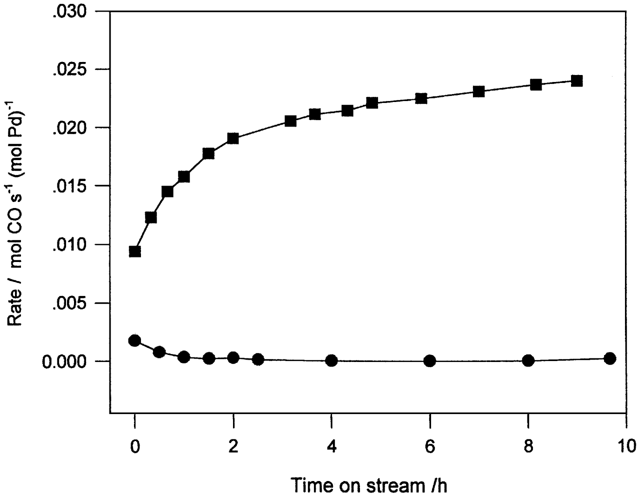

FIG. 7. The rate of CO oxidation over $PdCl_2$–$CuCl_2$–$Cu(NO_3)_2/Al_2O_3$ catalyst containing 2 wt% Pd and 12 wt% Cu($[CuCl_2]:[Cu(NO_3)_2] = 1:2$) at different temperatures of 318 K (●) and 373 K (■). The reactants, CO, O_2, and H_2O, were fed to the catalyst at a concentration of 1, 10, and 2.3 vol% each in nitrogen.

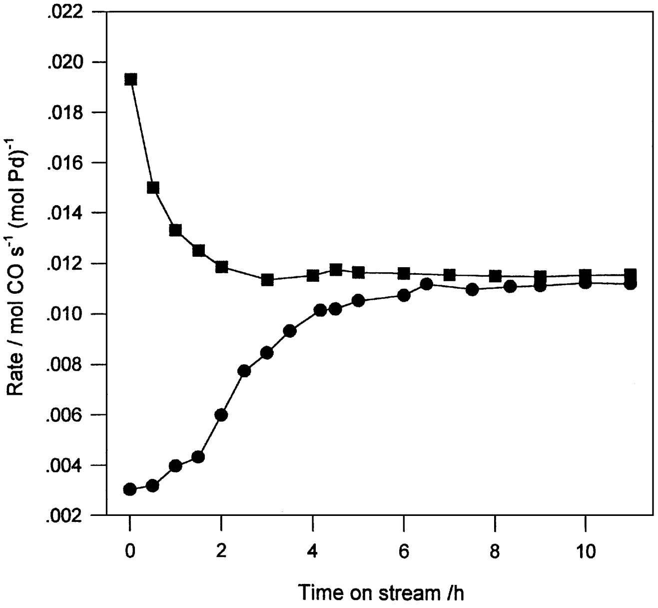

FIG. 9. The rate of CO oxidation over $PdCl_2$–$Cu(NO_3)_2$/carbon catalyst containing 2 wt% Pd and 6 wt% Cu at different temperatures of 303 K (●) and 423 K (■). The reactants, CO, O_2, and H_2O, were fed to the catalyst at a concentration of 1, 10, and 2.3 vol% each in nitrogen.

Effects of HCl and SO_2 on the Catalyst Deactivation

The effect of HCl on CO oxidation over carbon-supported $PdCl_2$–$CuCl_2$–$Cu(NO_3)_2$ catalyst was tested. When 37 and 74 ppm of HCl were added in the feed, the steady-state CO conversion decreased from 0.9 to 0.83 and 0.36, respectively. SO_2 deactivated this catalyst more severely, although catalytic activity was restored to some extent after the SO_2 feeding was stopped, as shown in Fig. 11. XRD patterns of this catalyst after CO oxidation shown in Fig. 12 indicate only peaks due to carbon support. Apparently HCl and SO_2 inhibited the formation of the $Cu_2Cl(OH)_3$ phase. In order to identify these noncrystalline phases, which are invisible with XRD, XANES was employed. The Cu *K*-edge

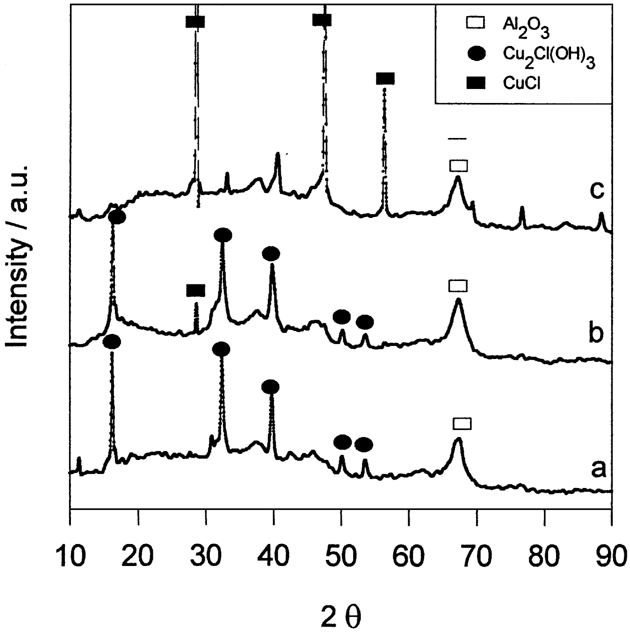

FIG. 8. X-ray diffractogram of $PdCl_2$–$CuCl_2$–$Cu(NO_3)_2/Al_2O_3$ catalysts before reaction (a), after reaction at 373 K (b), and after reaction at 318 K (c).

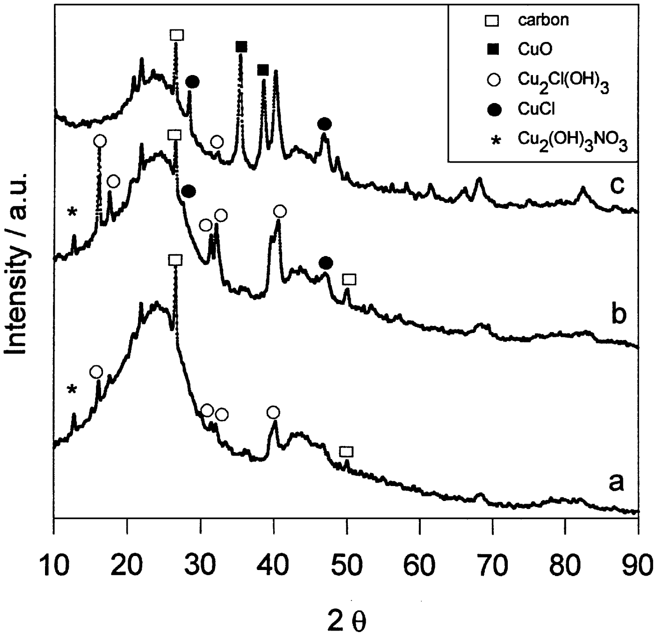

FIG. 10. X-ray diffractogram of $PdCl_2$–$Cu(NO_3)_2$/carbon catalysts before reaction (a), after reaction at 303 K (b), and after reaction at 423 K (c).

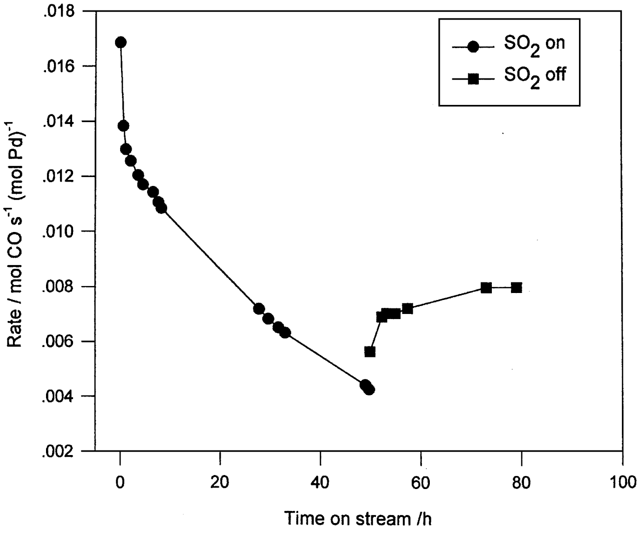

FIG. 11. Effects of SO_2 on the rate of CO oxidation over $PdCl_2$–$CuCl_2$–$Cu(NO_3)_2$/carbon catalyst containing 1.7 wt% Pd and 6 wt% Cu($[CuCl_2]:[Cu(NO_3)_2]=1:1$) at 313 K. The reactants, CO, H_2O, and SO_2, were fed to the catalyst at a concentration of 1 vol%, 2.3 vol%, and 258 ppm each in air.

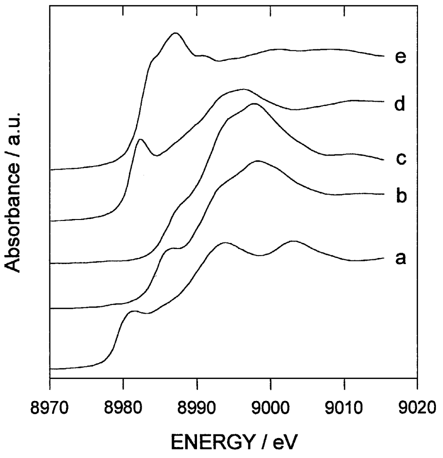

FIG. 13. Copper *K*-edge XANES of Cu references: Cu foil (a), CuO (b), $Cu(OH)_2$ (c), Cu_2O (d), CuCl (e).

XANES are compared in Figs. 13a–13e for Cu foil, CuO, $Cu(OH)_2$, Cu_2O, and CuCl, respectively, as references. As discussed elsewhere (13, 14, 20, 21), the absorbance maximum is assigned to the allowed $1s \rightarrow 4p$ transition. Below the maximum are subsidiary peaks and shoulders reflecting transitions to empty orbitals according to the dipole selection rule. The small peak at 8981 eV in Figs. 13a and 13d is due to the $1s \rightarrow 4s$ transition. This peak is expected for Cu(0), which has an empty 4*s* orbital. The presence of the sharper peak in Cu_2O reflects the tendency of the Cu(I) compound to assume trigonal or distorted tetrahedral geometry which allows *s*-*p* mixing (13, 14, 20, 21). A very weak peak below the edge at 8978 eV in CuO and $Cu(OH)_2$ represents the quadruple-allowed $1s \rightarrow 3d$ transition, which serves as a signature of a Cu(II) compound since there is no 3*d* hole in Cu(0) or Cu(I) compounds. The $1s \rightarrow 4s$ peak in Cu(II) compounds appears at 8985 eV as a shoulder with much reduced intensity. The edge positions of these references were determined to be 8979.0, 8984.6, 8986.3, 8981.0, and 8982.5 eV for Cu foil, CuO, $Cu(OH)_2$, Cu_2O, and CuCl, respectively, and again reflected the shift to a higher energy as the oxidation number was raised. According to XANES, both $PdCl_2$–$CuCl_2$–$Cu(NO_3)_2$/carbon catalysts before (Fig. 14a) and after reaction at 313 K (Fig. 14b) contained Cu(II) species. Yet, both catalysts showed a broad maximum in absorbance, unlike any other reference copper compounds. General features of these XANES spectra are similar to those previously observed for $PdCl_2$–$CuCl_2$/Al_2O_3 catalysts that were active in CO oxidation, except the doublet maxima for the latter (13, 14) instead of one broad maximum as observed here.

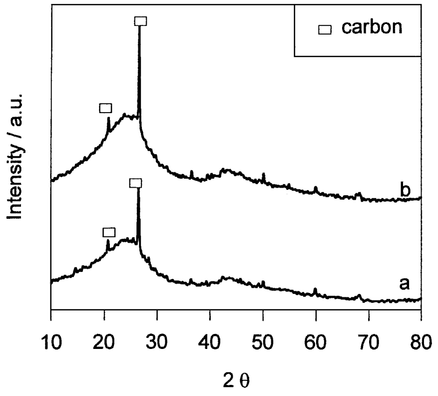

FIG. 12. X-ray diffractogram of $PdCl_2$–$CuCl_2$–$Cu(NO_3)_2$/carbon catalysts after reaction at 313 K in the presence of HCl (a) and after reaction at 313 K in the presence of SO_2 (b).

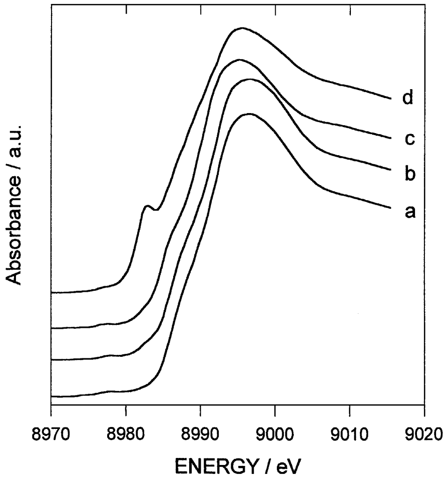

FIG. 14. Copper *K*-edge XANES of $PdCl_2$–$CuCl_2$–$Cu(NO_3)_2$/carbon catalysts: before reaction (a), after reaction at 313 K (b), after reaction at 313 K in the presence of HCl (c), and after reaction at 313 K in the presence of SO_2 (d).

The spectrum was assigned to $Cu_2Cl(OH)_3$. XANES spectra of this catalyst after poisoning with HCl (Fig. 14c) and SO_2 (Fig. 14d) show changes in the shape of spectra and edge positions. The edge positions of these samples were determined to be 8986.4, 8986.3, 8984.9, and 8981.4 eV for Figs. 14a–14d, respectively. The shift in edge positions of the deactivated catalysts to lower energies indicated that the oxidation number of copper in these catalysts was reduced. Furthermore, there was a well-defined peak at 8982 eV due to $1s \rightarrow 4s$ transition in XANES of the catalyst deactivated by SO_2, indicating the presence of reduced copper species.

DISCUSSION

The effects of supports, $Cu(NO_3)_2$ addition, and the presence of poisoning gases such as HCl and SO_2 on CO oxidation over Wacker-type catalyst were examined at different temperatures. A remarkably consistent relation between the Cu phase and the catalytic activity was observed. Active catalysts under various reaction conditions that give rise to good activities always showed a well-developed $Cu_2Cl(OH)_3$ phase observed by XRD. Other copper phases, $CuCl_2$, CuCl, or CuO, were found to be unstable or inactive. In all cases, XRD did not show any palladium phase, in agreement with our previous finding that palladium remains a molecular species in these catalysts (13, 14).

The catalytic cycle of Wacker chemistry appears to be stable over alumina- and carbon-supported $PdCl_2$–$CuCl_2$ catalysts. However, the last step, reoxidation of CuCl, does not seem to be achieved over silica. The irreversible transformation of the copper phase into CuCl means a decrease in the amount of the Cu(II) species that oxidizes the reduced Pd(0) species back to Pd(II) compounds, which are essential in oxidizing CO in the Wacker chemistry. This difference in stability is considered to be related to the surface characteristics of supports for stabilizing the active copper species, $Cu_2Cl(OH)_3$ (atacamite). H-type mordenite, having the characteristics of both alumina and silica, showed intermediate catalytic activity. For an identical support, the difference in the catalytic activity with increasing and decreasing reaction temperatures goes hand-in-hand with the change in XRD intensity of the $Cu_2Cl(OH)_3$ phase. Alumina, silica, and carbon are known to have the characteristic surface hydroxyl groups (22–24). Rouco (25) studied low-temperature ethylene oxyhydrochlorination over supported $CuCl_2$ catalysts and reported that $Cu_2Cl(OH)_3$ was present only over γ-Al_2O_3 and that $CuCl_2 \cdot 2H_2O$ was present over α-Al_2O_3 and SiO_2. The involvement of basic hydroxyl groups, abundant on γ-Al_2O_3 but not on the other two supports, has been suggested to be responsible for the preferred formation of $Cu_2Cl(OH)_3$ on γ-Al_2O_3 (26). Rouco (25) also observed from temperature-programmed reduction measurements that the peaks due to two-step reduction of the cupric species are shifted to higher temperatures for copper chloride supported on α-Al_2O_3 or SiO_2 compared to γ-Al_2O_3-supported copper chloride. Apparently, $Cu_2Cl(OH)_3$ is easier to reduce to cuprous species than $CuCl_2 \cdot 2H_2O$, and, therefore, the reduced Pd species can be reoxidized more easily by $Cu_2Cl(OH)_3$ to become active sites for CO oxidation in the supported Wacker-type catalysts.

In this study both hydrophilic supports such as alumina and silica and hydrophobic support such as carbon were employed. Therefore there is a possibility of pore-filling or capillary condensation in hydrophilic supports during reaction under wet conditions. However, the water content under our reaction conditions appears far lower than the content causing diffusion problems due to pore-filling because, as the water content increased further to more than 2.3%, the catalytic activity also increased. We also observed the same simple increase in catalytic activity with increasing water contents over both hydrophilic alumina and hydrophobic carbon. The result is not consistent with the result at low temperatures [10]. A strong and complicated dependency of activity on water content was observed for hydrophilic supports showing a maximum activity at an intermediate water content. On the other hand, there was virtually no dependence of the activity on the water content for the hydrophobic supports, although the presence of water was still required for CO oxidation to proceed. Thus, it appears that high temperatures have made the hydrophilic support less susceptible to pore-filling.

For carbon-supported $PdCl_2$–$CuCl_2$ catalysts, Yamamoto *et al.* (15) observed the partial reduction of cupric species and Pd(II) species and concluded that Pd metal particles were responsible for the low-temperature activities of CO oxidation at >400 K and that Cu(I) chloride species showed the activity only at >570 K. They used a low loading of Cu (1.2 wt%), compared with the 12 wt% Cu used in this work. Furthermore, there was no clue that thier catalysts had the low-temperature CO oxidation activity comparable to that of our catalysts. Desai *et al.* (8) and Kim *et al.* (10) reported that the CO oxidation activity increased with the amount of Pd and Cu in alumina-supported $PdCl_2$–$CuCl_2$ catalysts. For carbon-supported $PdCl_2$–$CuCl_2$ catalysts, the same phenomena were also observed (16). Therefore, the active copper phase defined by the Yamamoto group cannot be directly related to that in our carbon-supported $PdCl_2$–$CuCl_2$ catalysts, which show remarkably high CO oxidation activities even at low temperatures.

The addition of $Cu(NO_3)_2$ has been reported to enhance the catalytic activity for CO oxidation (6). We tested other Cu precursors, such as $Cu(OH)_2$, $Cu(CH_3COO)_2$, and $CuCO_3$-$Cu(OH)_2$ and their mixtures with $CuCl_2$. However, $Cu(NO_3)_2$ was found to be the most active promoter (11).

The carbon-supported $PdCl_2$–$CuCl_2$–$Cu(NO_3)_2$ catalyst showed a higher steady-state catalytic activity than the corresponding $PdCl_2$–$CuCl_2$ catalyst and the catalytic activity was directly related to the enhanced peak intensity of $Cu_2Cl(OH)_3$. However, there was an induction period at low temperatures. At high temperatures or when this catalyst was calcined at 473 K, the induction period disappeared and the strong $Cu_2Cl(OH)_3$ peak was observed initially. Mass spectroscopy analysis of the gaseous products generated during temperature-programmed oxidation of the catalyst showed the removal of NO and NO_2. Therefore the NO_3^- species appears to be removed in this induction period. The particle size of the Cu compound calculated from the application of the Scherrer equation to the (011) peak of $Cu_2Cl(OH)_3$ was 30 nm and did not change with the peak intensity. Hence, it appears that the increased catalytic activity was not related to the increased dispersion of Cu species in this catalyst system. The initial low activity can be explained by the presence of inactive $Cu(NO_3)_2$ species on $Cu_2Cl(OH)_3$ particles. However, these inactive species can be transformed into active $Cu_2Cl(OH)_3$ by removing NO_3^- during the induction period as described above.

To demonstrate a quantitative correlation between the catalytic activity and the peak intensity of the $Cu_2Cl(OH)_3$ phase, the rates of CO oxidation at 318 and 373 K were plotted against the peak height of the (011) plane of $Cu_2Cl(OH)_3$ in Fig. 15. Data used for the plot were derived from different catalyst compositions, supports, treatments, and reaction conditions. A significant correlation was observed, but the slope varied with the reaction temperature. There was some residual catalytic activity even without the $Cu_2Cl(OH)_3$ phase in XRD. However, no catalytic activity was observed over Pd-free catalysts even when the well-developed $Cu_2Cl(OH)_3$ phase was present. This indicates that Pd is the active species and $Cu_2Cl(OH)_3$ is its redox partner indispensable in the Wacker chemistry. As shown in Table 1 the peak intensity of the $Cu_2Cl(OH)_3$ phase was related somewhat to dioxygen pressure, but not to water pressure. Thus, it can be concluded that the formation of $Cu_2Cl(OH)_3$ is due mainly to the interaction between Cu precursors and the surface hydroxyl groups of supports. Water in feed does not play a direct role in the process. However, the presence of dioxygen is essential for restoring reduced Cu(I) species to Cu(II) species as required in Wacker chemistry. Thus, the weakened $Cu_2Cl(OH)_3$ phase in the dioxygen-free condition can be explained by the consumption of the phase for the reoxidation of Pd(0) to Pd(II), yet itself not being able to be restored due to the absence of dioxygen.

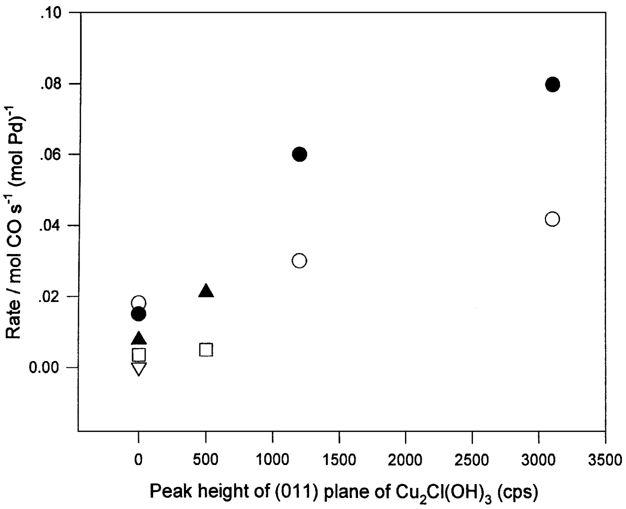

FIG. 15. The relation between the rate of CO oxidation and the peak height of the (011) plane of $Cu_2Cl(OH)_3$ phase in XRD patterns of catalysts used at 318 K (open symbols), and 373 K (closed symbols). The reaction conditions are the same as in Fig. 5. $PdCl_2$–$CuCl_2$–$Cu(NO_3)_2$/carbon at different times on stream (○, ●); $PdCl_2$–$CuCl_2$/carbon (▲); $PdCl_2$–$CuCl_2/Al_2O_3$ (□); $PdCl_2$–$CuCl_2$–$Cu(NO_3)_2$/carbon after SO_2 treatment (▽).

TABLE 1

Effect of Feed Compositions on the Peak Height of $Cu_2Cl(OH)_3$ in XRD Patterns[a]

Feed compositions $O_2(H_2O)$ in vol%	Peak height of (011) plane of $Cu_2Cl(OH)_3$[b] in cps
0.0 (4.2)	1800
10.0 (4.2)	2200
20.0 (4.2)	2100
10.0 (0.0)	2500
10.0 (1.7)	2300

[a] $PdCl_2$–$CuCl_2$–$Cu(NO_3)_2$/AC (2 wt% Pd, 12 wt% Cu) was treated with 1% CO, O_2, and H_2O in N_2 balance at 353 K for 10 h with space velocity (9000 L/hr kg cat.).

[b] Baseline corrected.

The alumina-supported $PdCl_2$–$CuCl_2$–$Cu(NO_3)_2$ catalyst showed decreasing activity at low temperatures in spite of the initial presence of the $Cu_2Cl(OH)_3$ phase. It was found that a part of the $Cu_2Cl(OH)_3$ phase transformed into the CuCl phase during the reaction. However, this catalyst showed increasing activity with reaction time at high temperatures. At these temperatures the stable $Cu_2Cl(OH)_3$ phase was restored. Thus, the stability of the $Cu_2Cl(OH)_3$ phase is temperature-dependent over Al_2O_3. Desai *et al.* (8) reported that CO conversion decreased with time over $PdCl_2$–$CuCl_2$– $Cu(NO_3)_2/Al_2O_3$ catalysts due to the loss of small amounts of HCl from the catalysts under the reaction condition, with consequent loss of activity for reoxidation of Pd(0) to Pd(II) and that prechlorination increased the catalyst stability significantly. His observation could also be explained by the stability of the $Cu_2Cl(OH)_3$ phase as described in this paper.

The carbon-supported $PdCl_2$–$Cu(NO_3)_2$ catalyst without $CuCl_2$ showed much lower activities of CO oxidation than $PdCl_2$–$CuCl_2$ catalysts. Hence, two copper precursors show a synergy in activity when they are present together. The $PdCl_2$–$Cu(NO_3)_2$ catalyst showed time-dependent activity at low temperatures that was again closely related to the change in copper phase. As described, the XRD intensity of the $Cu_2Cl(OH)_3$ phase was enhanced with time on stream at the low temperature with the concomitant increasing catalytic activity. The source of chlorine to form $Cu_2Cl(OH)_3$ is believed to be $PdCl_2$. At the high temperature, however, $Cu(NO_3)_2$ decomposed into CuO and the catalytic cycle of Wacker chemistry became ineffective, as indicated by extremely low CO conversions. Therefore it could be concluded that $Cu(NO_3)_2$ helps the formation of the active phase $Cu_2Cl(OH)_3$ which is stable at high temperatures and that the presence of both $CuCl_2$ and $Cu(NO_3)_2$ is essential for this synergy effect.

HCl and SO_2 are common air pollutants which are emitted with CO in the combustion of fuels containing sulfur and chlorine compounds. These are also well-known poisons to metal catalysts. Therefore their effect on our catalyst system is a necessary consideration in the practical application of CO oxidation processes.

The carbon-supported $PdCl_2$–$CuCl_2$–$Cu(NO_3)_2$ catalyst was deactivated to some extent by the presence of HCl in the feed and the loss of the catalytic activity became more serious when HCl concentration was higher. The deactivation by SO_2 was even more severe. X-ray diffraction showed that these gases inhibited the formation of the active $Cu_2Cl(OH)_3$ phase. No copper phase was observed by XRD in catalysts deactivated by HCl or SO_2. This tendency was also observed when HCl and H_2SO_4 were added during the preparation of the catalysts. Because Wacker-type catalysts were reported to oxidize SO_2 to H_2SO_4 in the presence of H_2O (6, 19), effects of H_2SO_4 addition during the catalyst preparation were examined. The addition of excess H_2SO_4 caused the appearance of the new solid phases such as $CuSO_4 \cdot 5H_2O$, $CuSO_4 \cdot H_2O$, and Cu_2SO_4. In order to probe the formation of a noncrystalline copper phase, XANES was employed because it should be sensitive to local bonding. According to the XANES, broad $1s \rightarrow 4p$ peaks representing the $Cu_2Cl(OH)_3$ phase were observed before and after the reaction with a clean feed at 313 K. However, peak shapes changed after poisoning by HCl and SO_2. These observations are consistent with XRD patterns that showed the disappearance of the $Cu_2Cl(OH)_3$ phase. The addition of HCl or SO_2 causes the shift of the Cu K-edge energy in XANES to lower values, indicating the reduction of copper species. In particular, the Cu K-edge energy of the catalyst deactivated by SO_2 is similar to those of reference Cu(I) compounds. The possible phase might be an amorphous Cu_2SO_4 phase because the phase was observed in XRD of catalysts to which H_2SO_4 was added during preparation.

CONCLUSIONS

The activity of supported Wacker-type catalysts in CO oxidation depends on the nature of support, the composition of copper precursors, the presence of poisons such as HCl and SO_2, and the reaction temperatures. This complicated behavior of the catalysts is closely related to the nature of the copper phase. All the above variables influencing the activity affected in a consistent manner the XRD intensity of the $Cu_2Cl(OH)_3$ phase which is believed to be the active copper phase. Thus, its XRD intensity is closely correlated with the catalytic activity and its behavior with respect to different reaction and preparation conditions is directly reflected in the change in catalytic activity of CO oxidation with respect to these variables.

REFERENCES

1. Yao, Y. Y., *J. Catal.* **87**, 152 (1984).
2. Brittan, M. I., Bliss, H., and Walker, C. A., *AIChE J.* **16**, 305 (1970).
3. Fuller, M. J., and Warwick, M. E., *J. Chem. Soc. Chem. Commun.* 210 (1973).
4. Haruta, M., Tsubota, S., Kobayashi, T., Kageyama, H., Genet, M. J., and Delmon, B., *J. Catal.* **144**, 175 (1993).
5. Boulahouache, A., Kons, G., Lintz, H.-G., and Schulz, P., *Appl. Catal. A* **91**, 115 (1992).
6. Lloyd, W. G., and Rowe, D. R., *Environ. Sci. Technol.* **5**(11), 1133 (1971).
7. Lloyd, W. G., and Rowe, D. R., U.S. Patent 3,790,662 (1974).
8. Desai, M. N., Butt, J. B., and Dranoff, J. S., *J. Catal.* **79**, 95 (1983).
9. Choi, K. I., and Vannice, M. A., *J. Catal.* **127**, 489 (1991).
10. Kim, K. D., Nam, I.-S., Chung, J. S., Lee, J. S., Ryu, S. G., and Yang, Y. S., *Appl. Catal. B* **5**, 103 (1994).
11. Koh, D. J., Song, J. H., Ham, S.-W., Nam, I.-S., Chang, R.-W., Park, E. D., Lee, J. S., and Kim, Y. G., *Korean J. Chem. Eng.* **14**(6), 486 (1997).
12. Lee, C. W., Park, S.-J., Kim, Y.-S., and Chong, P. J., *Bull. Korean Chem. Soc.* **16**(3), 296 (1995).
13. Lee, J. S., Choi, S. H., Kim, K. D., and Nomura, M., *Appl. Catal. B* **7**, 199 (1996).
14. Choi, S. H., and Lee, J. S., *React. Kinet. Catal. Lett.* **57**, 227 (1996).
15. Yamamoto, Y., Matsuzaki, T., Ohdan, K., and Okamoto, Y., *J. Catal.* **161**, 577 (1996).
16. Park, E. D., M.S. Thesis, Pohang University of Science and Technology, 1997.
17. Rehr, J. J., Mustre de Leon, J., Zabinsky, S. I., and Albers, R. C., *J. Am. Chem. Soc.* **113**, 5135 (1991).
18. Teo, B. K., "EXAFS: Basic Principles and Data Analysis." Springer-Verlag, Berlin, 1985.
19. Jumakaeva, B. S., and Golodov, V. A., *J. Mol. Catal.* **35**, 303 (1986).
20. Choi, E. Y., Nam, I., Kim, Y. G., Chung, J. S., Lee, J. S., and Nomura, M., *J. Mol. Catal.* **69**, 247 (1991).
21. Brown, J. M., Powers, L., Kincaid, B., Larrabee, J. A., and Spiro, T. G., *J. Am. Chem. Soc.* **102**, 4210 (1980).
22. Knozinger, H., and Patnasamy, P., *Catal. Rev. Sci. Eng.* **17**(1), 31 (1978).
23. Iler, R. K., "The Chemistry of Silica: Solubility, Polymerization, Colloid and Surface Properties, and Biochemistry." Wiley, New York, 1979.
24. Bansal, R. C., Donnet, J.-B., and Stoeckli, F., "Active Carbon." Dekker, New York, 1988.
25. Rouco, A. J., *J. Catal.* **157**, 380 (1995).
26. Zipelli, C., Bart, J. C., Petrini, G., Galvagno, S., and Cimino, C., *Z. Anorg. Allg. Chem.* **502**, 199 (1983).